Fibers and Polymers 2017, Vol.18, No.10, 1931-1937
DOI 10.1007/s12221-017-7042-x

ISSN 1229-9197 (print version)
ISSN 1875-0052 (electronic version)

Muscle Activity Monitoring with Fabric Stretch Sensors

Chicuong Vu and Jooyong Kim*

Department of Organic Materials and Fiber Engineering, Soongsil University, Seoul 06978, Korea
(Received January 12, 2017; Revised July 21, 2017; Accepted July 25, 2017)

Abstract: In this paper, development of a fabric stretch sensor embedded system has been proposed for muscle activity monitoring. It is expected that this product will be proper for monitoring a wide range of human activities mainly due to the characteristics of light-weight and high sensitivity. The fabric sensors developed can be easily attached to almost any types of clothing due to their thin and stretchable natures. The mechanism and performance of the sensors have been characterized by measuring the mechanical and electrical performance along with stretch ratio or strain percent. The data collected would be successfully transmitted to mobile phones through low power consumption BLE connection, and thus muscle activities in real time. As expected, the resultant smart muscle pants could achieve realistic goals through monitoring body movements without any significant loss of wear comforts in normal clothing. This work significantly contributed in enhancing the utility of strain/stretch sensors for development of e-textiles and intended to be a starting point for data collection and analysis of smart fabric embedded sensing technologies.

Keywords: Single-walled carbon nanotubes (SWCNT), Polyethylene terephthalate (PET), Electronic textile, Wearable devices, Strain sensor, Motion sensing, Contact resistance, High sensitivity, Gauge factor, Hysteresis, Current-voltage curves (I-V)

Introduction

Recent soft sensor applications [1] have focused on revealing the multi-dimensional aspects of human life, the way of moving and interacting with surrounding environment [2]. In particular, sports and healthcare [3], motion analysis [4] is one of the most important applications from which we may construct plans for training, tactics or health monitoring [5,6]. However, traditional electronic devices are not suitable for long term/continuous monitoring or inconvenient/mal-functional while moving. In addition, low durability of electrodes and circuits on skin is another obstacle. As a promising technology, *e*-textiles by combining textiles and electronics have been expected to play an important role in development of smart materials capable of accomplishing the corresponding function, found in rigid and non-flexible electronic products in the past. The concept "fabric strain sensor" [7-11] was developed as one of the methods to detect signals with a wide range of applications in parameters based on the change in resistance values to detect body movements [12]. There have been many attempts to make strain sensor [13] and develop on wearable devices [14] which can be directly attached to the skin [15]. Most of strain sensors are to use resistive-type sensors or capacitive-type sensors due to their relatively simple structure and fabrication process, low energy consumption in operation [16,24]. The fabric strain sensors could have different structures by interlacing sensing fibers with non-sensing fibers or by applying a coating with strain sensing materials to achieve the same goal. Flexible resistive-type strain sensors could be fabricated by embedding soft elastomeric materials into conducting fillers [22,25], such as: gold and silver nanowires [17,18], carbon nanotubes [19,20], and graphene [21,23,28-35]. Conductive Polyethylene terephthalate (PET) fabrics were prepared by padding conductive ink (Single-walled carbon nanotubes-SWCNT [26,27]), in order to construct two-dimensional textile sensors. Based on that method, this paper proposed a fabric strain sensor which is extremely thin, lightweight, sensitive, and thus high level of flexibility.

*Corresponding author: jykim@ssu.ac.kr

Experimental

Textile Sensor

Sensor Design

PET/Spandex (PET/SP) fabric is widely used in the industry to produce products such as clothing, household furniture, industrial fabrics. In order to make the perfect

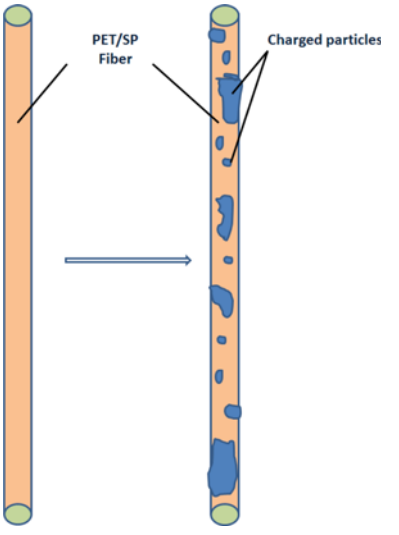

Figure 1. Schematics of the PET/SP fabric strain sensor.

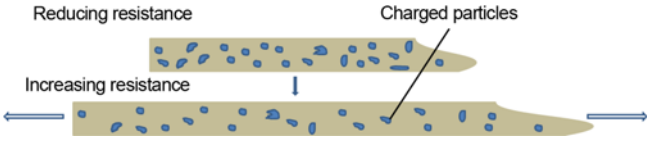

Figure 2. Fabric strain sensor changes resistance when straining.

product for sweat, dust protection applications. The PET/SP fabric is inherently composed of conventional PET/SP multifilament yarns with high elasticity. The PET/SP fibers could be converted into carbon fiber via coating and surface treatment. In order to fabricate the fabric sensor, carbon powder ink was applied by water-based single-walled carbon nanotube solution (SWCNT dispersed ink in H_2O) with nanotubes with 1.0-1.3 nm diameter and 0.1 wt% concentration.

The strain sensor was based on the change in electrical resistance in sensor layer along with stretch (Figure 2). For making the fabric type with carbon particles, we used stretchable fabric (PET:Spandex=76:24, Item 16043A, 341 g/YD, 262 g/SQM, from SNT company, South Korea Co. Ltd.) and SWCNT solution. Conductive ink was made of 0.1wt% SWCNT and dispersant based on water. The SWCNT raw powder (KH CHEMICAL Co. Ltd., South Korea) was prepared and treated by acid solution (HNO_3: H_2SO_4=3:1). And then, we put it into the water with dispersant, SDBS (Sodium Dodecyl-benzenesulfonate). After mixing with Stirring machine (60-80 ^oC, 1000 RPM, 24 hr), the solution was treated with Ultra-sonificator (2 hr, 19,990 Hz). In this paper, the dipping and drying process were performed by Automatic dipping padding machine and textile two-way drying machine (DAELIM STARLET Co. Ltd., South Korea).

First, the PET/SP fabric contained stretchable fabrics prepared and immersed in SWCNT ink within the bath of the Dipping machine. The impregnating process would keep the conditions that allow the SWCNT particles to penetrate well (Pressure roll speed 1.0 m/min, Air cylinder pressure: 3 bar (0.3 MPa) over). This process would make the SWCNT particles adhere the stretchable fabric after dipping and squeezing. And then, the Textile drying machine with two-way wind type was used to get rid of the excessive water in

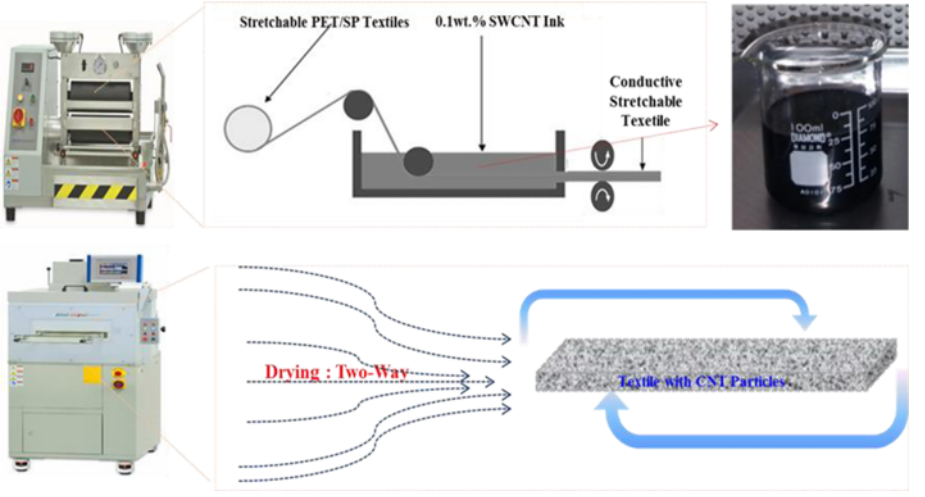

Figure 3. The machines for making the textile strain sensor.

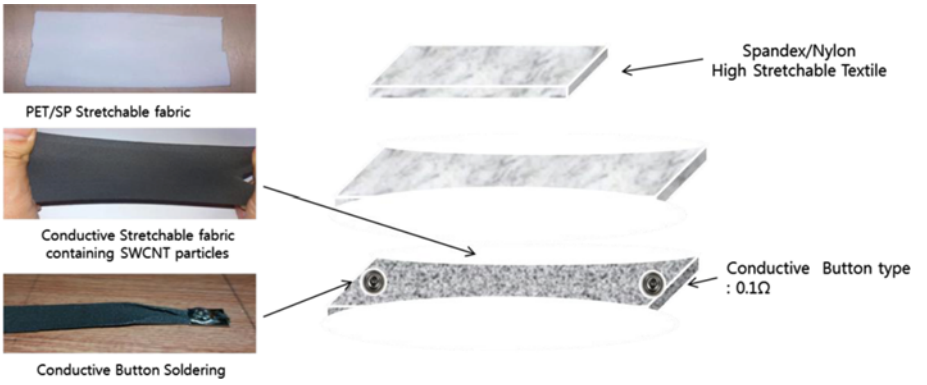

Figure 4. Conductive strain textile sensors.

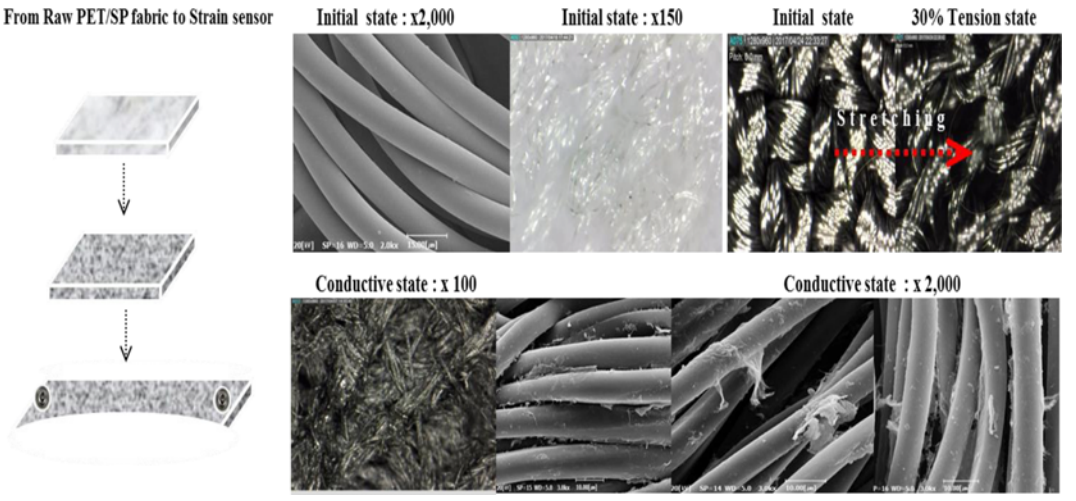

Figure 5. SEM & Microscope images of the conductive strain textile sensor.

the stretchable fabric. At this point, vacuum dried under fixed condition (Dry time: 1-3 mins, Temperature range: 180-200 °C, Circulation Fan Speed: 1500 RPM/min) was optimized (Figure 3).

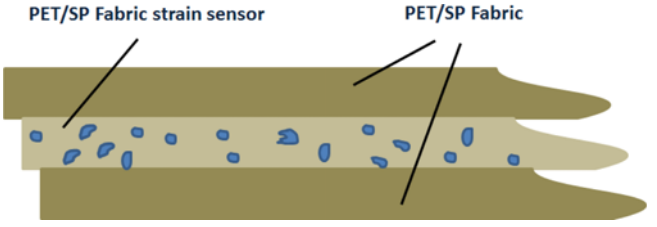

Figure 6. 3-layer structure of the fabric strain sensor.

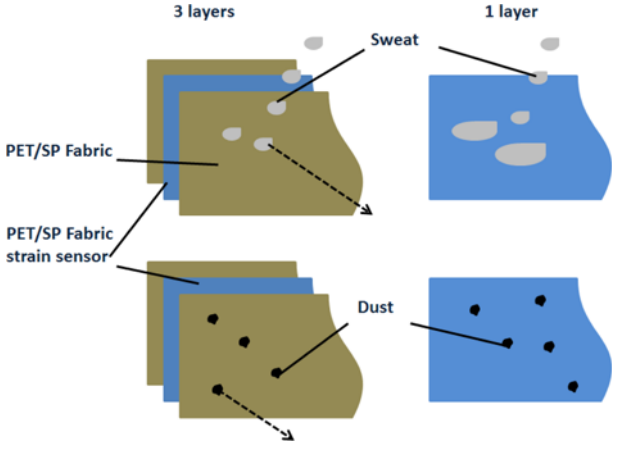

Figure 7. Difference between two structures: 3 layers and 1 layer.

The PET/SP fabric strain sensor could be conductive fabrics after dipping process with SWCNT Ink. The single layer-conductive strain fabrics made were examined by SEM (scanning electron microscope) (Figure 4, 5). When checking the SEM images, the SWCNT particles were observed between yarns, revealing that CNT particles were adhered to the surface of the fiber axis.

In the case of a single-layer textile sensor, the simple layer is not only susceptible to damage from other dust, moisture, and external substances, but also has difficulty in maintaining the performance of the sensor itself. 30 μm thick PU based films with very low modulus were attached by thermal pressing on both sides of the fabric in order to protect the fabric from abrasion, dusts and sweets. This 3 layers structure has been finally chosen in order to ensure good stretchability, elastic recovery and comfort for user (Figure 6, 7). Two outer layers provide protection and durability without any significant loss of measurement characteristics such as resolution and stretchability. The abrasion resistance performed under KS K0650 clearly revealed that the abrasion durability was enough for realistic applications. Resulting fabric surface was kept intact after 30000 abrasion cycles.

Circuit Design

The resistance of strain sensor will be changed in very sensitive manner along with body movements. Processing circuits and devices are needed in order to measure, process and send the series of data in real time The data acquisition and conversion system as shown below:

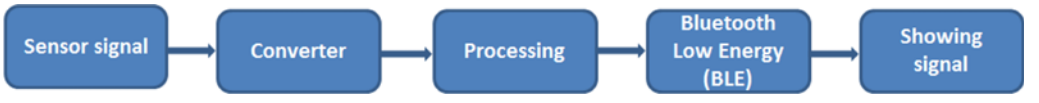

Figure 8. Diagram of circuit design for sensor signals.

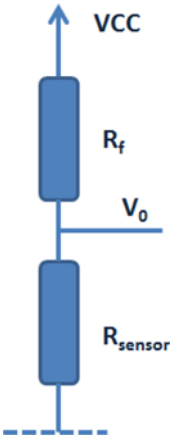

Figure 9. Voltage divider circuit.

Resistance Measurement

Measurement Electronics

The method used to monitor activities is based on the relationship between mechanical and electrical properties of constituent conductive fabrics. Using a voltage divider circuit (Figure 9), the resistance variation has been converted into a voltage variation as follows:

Data of the voltage was sampled/digitized and thus converted into the digital values. For resolution reason, mathematical mapping of voltage values between 0 to 3.7 volts into digital values between 0 to 1023 (3.7/1023= 0.0037 volt or 3.7 mV per unit) has been made by pre-calculating the actual data. It was calculated to take about 0.01 s (10 ms) to read an analog signal input, and maximum reading is about 100 times per second. The output voltage was calculated as follows:

$$V_0 = \frac{VCC}{R_{sensor} + R_f} R_f$$

The reference resistor (R_f) was optimized according to the actual resistance data of the sensor.

Results and Discussion

Structure of Fabric Strain Sensor

As shown in Figure 10, SEM shows that the width of the filaments is 10 μm, and loosely twisted and ample of free space between the microfiber bundles. It could be observed the coatings, which were created by charged particles, stuck randomly to PET/SP fibers. The electrical conductivity of initial resistance of the fabric strain sensor was shown in Figure 11. It is small and fit to measure easily (R~5 kΩ).

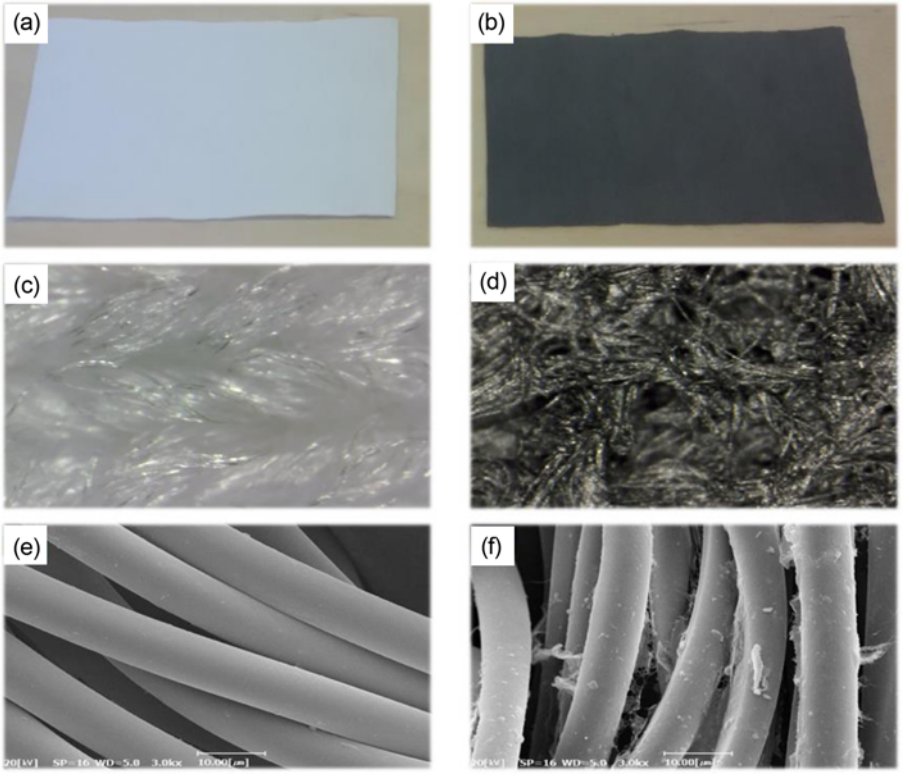

Figure 10. PET/SP fabric before and after applying carbon powder ink: (a) the initial PET/SP fabric (low-magnification images), (b) the PET/SP fabric strain sensor (low-magnification images), (c) the initial structure PET/SP fabric (Average-magnification images), (d) the structure PET/SP fabric strain sensor (average-magnification images), (e) the initial structure PET/SP fabric (high-magnification images), and (f) the structure PET/SP fabric strain sensor (high-magnification images).

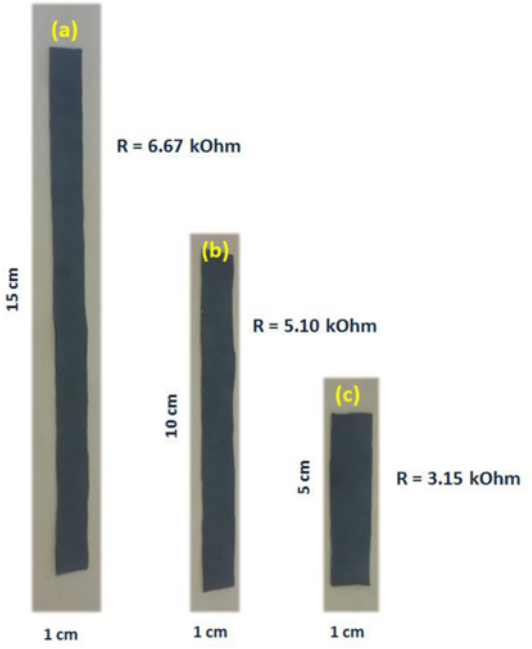

Figure 11. The initial resistance of fabric strain sensor at: (a) 5 cm, (b) 10 cm, and (c) 15 cm.

Electrical Properties of Fabric Strain Sensor

Current-Voltage Curves

The I-V curves, which is short for current-voltage characteristic curves, are a set of graphical curves which are used to define operation of the sensor within system. The I-V curves of fabric strain sensor under different static strains from 0-50 % were shown in Figure 12. As expected, the curves were linear in the voltage range of -2 to 2 V, which indicated the resistance of sensor was constant with an Ohmic behavior. The slope of the I-V curves reduced with an increase of applied strain, from 0-12.5-25-37.5 and 50 %, indicating that an increase in applied strain leaded to an increase in the sensor's resistance.

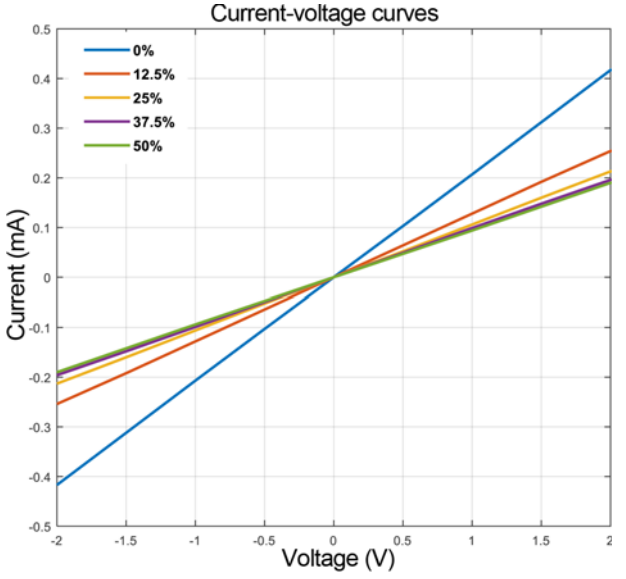

Figure 12. Current-voltage (I-V) characteristic curves.

Gauge Factor

The geometry of strain sensor fabrics has been determined in order to maximize the sensitivity through evauating the gauge factor. Multiple line structures have been known to be better in sensitivity and resolution compared to the single line design especially under the small deformation such as human muscle movement. The resistance-strain characteristics of the fabric strain sensor were shown in Figure 13. It is clear that the resistance increases along with the strain increases, and vice versa. When strained, the resistance of fabric sensor would initially increase and then decrease

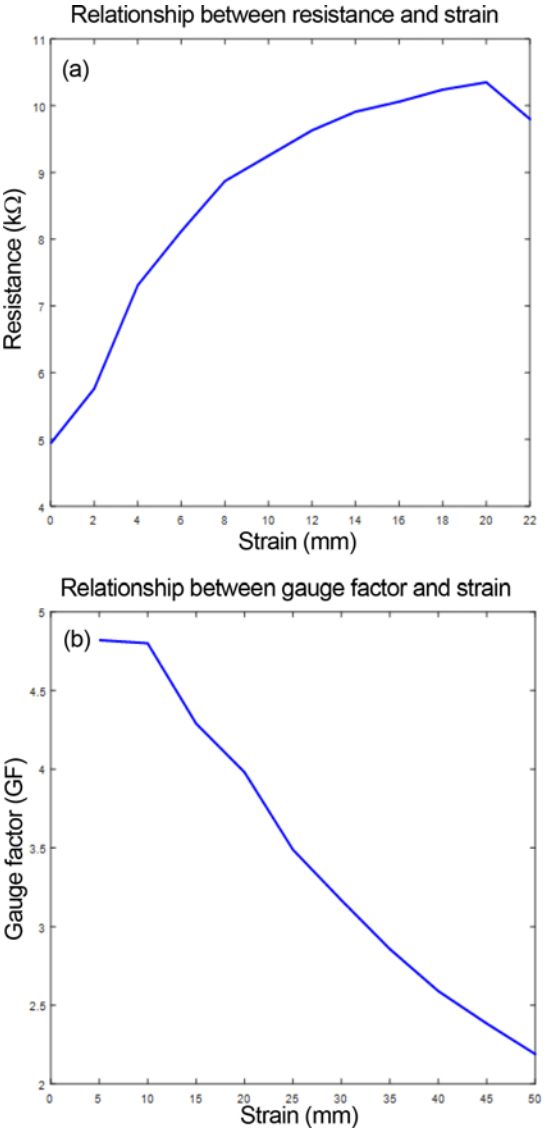

Figure 13. The resistance-strain relationship of fabric strain sensor; (a) resistance-strain and (b) gauge factor-strain.

(Figure 13(a)). The initial increase in resistance was due to the length increased, the gaps between the charged particles of fiber also increased. However, in the decreasing resistance phase, the gaps between the strands of fibers reduced, allowing better contact adding parallel conductivity paths which results in a lowered resistance. The gauge factor (GF) of a resistor defined as the ratio of a relative change in resistance ($\Delta R/R$) and strain (ε) was defined by using the equation as follows:

$$GF = \frac{\Delta R/R}{\Delta L/L} = \frac{\Delta R/R}{\varepsilon}$$

$$\varepsilon = strain\ (\%)$$

The results show that the gauge factor ranges from 2.19 to 4.82, and depends on the strain (%). As calculated gauge factor value, the strain sensor displayed high sensitivity.

Hysteresis

A system with hysteresis is defined as a system whose output does not only depend on the current input but also on the history of the input. Typical causes for the hysteresis are visco-elasticity and yarn friction in the fabric. The hysteresis increases with the decrease of the electrical resistance, which determines the number of contact points within a given length of fabric. The hysteresis behaviors are shown in Figure 14, indicating a linear rise in resistance when applying strain and only a small hysteresis.

Muscle Activity Measurement

The processing circuit digitizes and sends motion data signals from the sensor in order to arrange them into a custom format and transmit it via Bluetooth to mobile phone

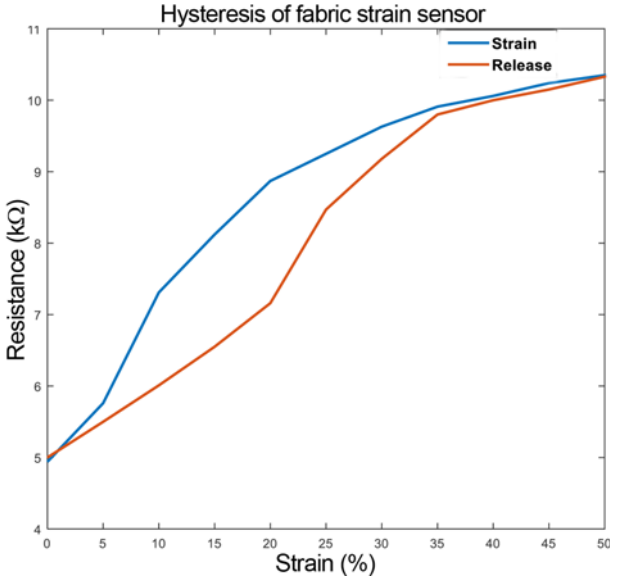

Figure 14. The typical resistance and strain for hysteresis error of fabric sensor.

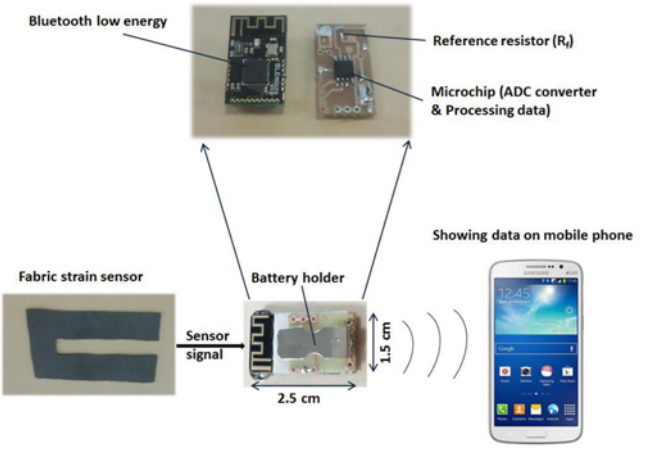

Figure 15. The strain sensor and operation principle in our experiment.

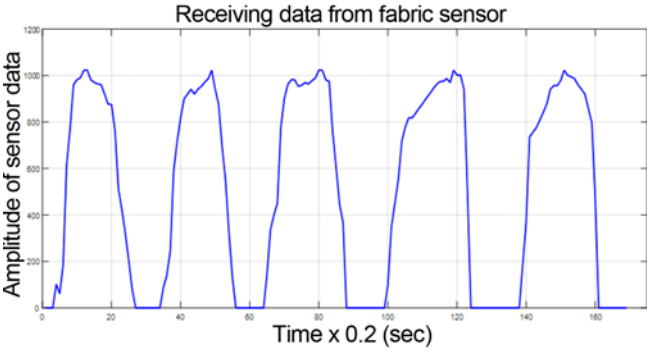

Figure 16. Data from the leg when lifting up and lowering down.

or tablet device in real time. A smartphone application has been developed to get data via Bluetooth connection. This application displays muscle activity data in series and reveals the features such as balance and distribution of muscle movement. The good thing about this system is that it emits low energy signals and the dimension of circuit is small: 1.5×2.5 cm (Figure 15), so the transmission of data should not and will not affect user. The operation system as shown below:

As shown in Figure 16, a plot of activity recognition experiments was presented with combination of a series of leg lifting and lowering motions. The variations of strain/stretch sensor have been proven to be consistent with actual movement patterns. The results have shown the feasibility of the strain/stretch fabric sensor with more accurate measurements of muscle activity than standard motion capture methods.

Conclusion

This paper has presented a fabric stretch sensor embedded muscle activity monitoring system and showed its potential for body motion recognition. The fabric strain sensor was

integrated into muscle pants in order to detect muscle activity on the thigh in particular. The future step of this study will be toward into implementation of the sensor for more detailed motion tracking and recognition. For this purpose, sensor arrays with 3-5 sensing elements will be employed so that the finding the best sensing area on the muscle can be implemented in order to make initial configuration in easier and quicker way. In addition, new algorithms will also be applied in order to process data with a higher level of accuracy. Accordingly optimal algorithms and devices need to be experimented in development and evaluation of smart clothing products.

Acknowledgement

The research was supported by Soongsil University.

References

1. S. Patel, H. Park, P. Bonato, L. Chan, and M. Rodgers, *J. Neuroeng Rehabil.*, **9**, 1743 (2012).
2. P. F. Binkley, *IEEE Eng. Med. Biol. Mag*., **22**, 23 (2003).
3. V. Custodio, F. J. Herrera, G. Lopez, and J. I. Moreno, *Sensors*, **12**, 13907 (2012).
4. O. Amft, H. Junker, P. Lukowicz, G. Troster, and C. Schuster, *Proc. BSN'06*, **48**, 138 (2006).
5. J. Farringdon, A. J. Moore, N. Tilbury, J. Church, and P. D. Biemond, *IEEE 3rd Int. Symp. Wearable Computers*, **6**, 107 (1999).
6. Y. Enokibori, Y. Ito, A. Suzuki, H. Mizuno, Y. Shimakami, T. Kawabe, and K. Mase, *Proc. UbiComp'13*, **P56**, 203 (2013).
7. L. M. Castano and A. B. Flatau, *Smart Mater. Struct.*, **23**, 53001 (2014).
8. C. Mattmann, F. Clemens, and G. Troster, *Sensors*, **8**, 3719 (2008).
9. Y. Enokibori and K. Mase, *IEEE 18th Int. Symp. Wearable Computers*, **9**, 129 (2014).
10. M. Pacelli, G. Loriga, N. Taccini, and R. Paradiso, *Proc. 3rd IEEE/EMBS Int. Summer School Symp. Med. Dev. Biosens.*, **10**, 1 (2006).
11. M. G. Urdaneta, R. Delille, and E. Smela, *Adv. Mater.*, **19**, 2629 (2007).
12. C. Cochrane, V. Koncar, M. Lewandowski, and C. Dufour, *Sensors*, **7**, 473 (2007).
13. I. Hirata, H. Nakamoto, H. Ootaka, and M. Tada, *Proc. 6th AHFE*, **3**, 845 (2015).
14. M. Stoppa and A. Chiolerio, *Sensors*, **14**, 11957 (2014).
15. V. J. Lumelsky, M. S. Shur, and S. Wagner, *IEEE Sensors J.*, **1**, 41 (2001).
16. W. Yi, Y. Wang, G. Wang, and X. Tao, *Polym. Test.*, **31**, 677 (2013).
17. S. Gong, W. Schwalb, Y. W. Wang, Y. Chen, Y. Tang, and J. Si, *Nat. Commun.*, **5**, 3132 (2014).
18. M. Amjadi, A. Pichitpajongkit, S. Lee, S. Ryu, and I. Park, *ACS Nano*, **8**, 5154 (2014).
19. S. Ryu, P. Lee, J. B. Chou, R. Xu, R. Zhao, and A. J. Hart, *ACS Nano*, **9**, 5929 (2015).
20. S. Li, J. G. Park, S. Wang, R. Liang, C. Zhang, and B. Wang, *Carbon*, **73**, 303 (2014).
21. H. Tian, Y. Shu, X. F. Wang, M. A. Mohammad, Z. Bie, and Q. Y. Xie, *Sci. Rep.*, **5**, 8603 (2015).
22. S. Jung, J. H. Kim, J. Kim, S. Choi, J. Lee, and I. Park, *Adv. Mater.*, **26**, 4825 (2014).
23. Y. A. Samad, Y. Li, S. M. Alhassan, and K. Liao, *ACS Appl. Mater. Interfaces*, **7**, 9195 (2015).
24. X. Liao, Z. Zhang, X. Yan, Q. Liang, and Q. Wang, *Adv. Funct. Mater.*, **26**, 3074 (2016).
25. B. Su, S. Gong, Z. Ma, L. W. Yap, and W. Cheng, *Small*, **11**, 1886 (2015).
26. C. Roman, T. Helbling, and C. Hierold, "Springer Handbook of Nanotechnology", pp.403-425, Springer Berlin Heidelberg, Germany, 2010.
27. J. Meyer, P. Lukowicz, and G. Troster, *IEEE 10th Int. Symp. Wearable Computers*, **11**, 69 (2006).
28. J. Lee, H. Kwon, J. Seo, S. Shin, J. H. Koo, C. Pang, S. Son, J. H. Kim, Y. H. Jang, D. E. Kim, and T. Lee, *Adv. Mater.*, **27**, 2433 (2015).
29. C. L. Choong, M. B. Shim, B. S. Lee, S. Jeon, D. S. Ko, T. H. Kang, J. Bae, S. H. Lee, K. E. Byun, J. Im, Y. J. Jeong, C. E. Park, J. J. Park, and U. I. Chung, *Adv. Mater.*, **26**, 3451 (2014).
30. J. Molina, J. Fernandez, A. I. del Rio, J. Bonastre, and F. Cases, *Appl. Surf. Sci.*, **279**, 46 (2013).
31. J. Molina, J. Fernandez, J. C. Ines, A. I. del Rio, J. Bonastre, and F. Cases, *Electrochim. Acta*, **93**, 44 (2013).
32. I. A. Sahito, K. C. Sun, A. A. Arbab, M. B. Qadir, and S. H. Jeong, *Carbohydr. Polym.*, **96**, 190 (2013).
33. L. Qu, M. Tian, X. Hu, Y. Wang, S. Zhu, X. Guo, G. Han, X. Zhang, K. Sun, and X. Tang, *Carbon*, **80**, 565 (2014).
34. K. Javed, C. M. A. Galib, F. Yang, C. M. Chen, and C. Wang, *Synth. Met.*, **193**, 41 (2014).
35. S. Pei, J. Zhao, J. Du, W. Ren, and H. M. Cheng, *Carbon*, **48**, 4466 (2010).